

# The importance of a surface organic layer in simulating permafrost thermal and carbon dynamics

Elchin Jafarov<sup>1</sup> and Kevin Schaefer<sup>1</sup>

<sup>1</sup> National Snow and Ice Data Center, Cooperative Institute for Research in Environmental Sciences, University of Colorado at Boulder, Boulder, CO 80309

\*Corresponding author, Email: elchin.jafarov@colorado.edu

## Abstract

Permafrost-affected soils contain twice as much carbon as currently exists in the atmosphere. Studies show that warming of the perennially frozen ground could initiate significant release of the frozen soil carbon into the atmosphere. To reduce the uncertainty associated with the modeling of the permafrost carbon feedback it is important to start with the observed soil carbon distribution. We initialized frozen carbon using the recent Northern Circumpolar Soil Carbon Dataset. To better address permafrost thermal and carbon dynamics we implemented a dynamic surface organic layer with vertical carbon redistribution, and introduced dynamic root growth controlled by active layer thickness, which improved soil carbon exchange between frozen and thawed pools. These changes increased the amount of simulated frozen carbon for present conditions from 313 to 560 GtC, which is more consistent with the observed frozen carbon stock.

## 1. Introduction

Warming of the global climate will lead to widespread permafrost thaw and degradation with impacts on ecosystems, infrastructure, and emissions to amplify climate warming (Oberman, 2008; Callaghan et al., 2011, Shuur et al., 2015). Permafrost-affected soils in the high northern latitudes contain  $1300 \pm 200$  Gt of carbon, where about 800 Gt C is preserved frozen in permafrost

Kevin Schaefer 12/3/2015 1:14 PM  
**Comment [1]:** Change to your new affiliation

Elchin Jafarov 11/16/2015 9:08 PM  
**Deleted:** . In addition  
Elchin Jafarov 11/16/2015 9:08 PM  
**Deleted:** we

Elchin Jafarov 12/19/2015 5:35 PM  
**Deleted:** amount of 550 GtC

Kevin Schaefer 12/3/2015 1:21 PM  
**Deleted:** These model developments improve the present day soil carbon distribution and thaw depth. Simulated amount of the present permafrost carbon stock was equal to 560 GtC Our results indicate that a dynamic surface organic layer improved permafrost thermal dynamics and simulated thaw depth. in oppose to 333GtC simulated by previous version of the.

Elchin Jafarov 11/16/2015 9:23 PM  
**Deleted:** These improvements allowed us achieve better agreement with the estimated carbon stocks in permafrost-affected soils using historical climate forcing.

40 | with ~550 GtC in the top three meters of soil (Hugeluis et al., 2014). As permafrost thaws,  
41 organic matter frozen within permafrost will thaw and decay, which will initiate the permafrost  
42 carbon feedback (PCF), releasing an estimated 120±85 Gt of carbon emissions by 2100  
43 (Schaefer et al., 2014). The wide range of estimates of carbon emissions from thawing  
44 permafrost depend in large part on the ability of models to simulate present permafrost area  
45 extent (Brown et al., 1997). For example, the simulated permafrost in some models is  
46 significantly more sensitive to thaw, with corresponding larger estimates of carbon emissions  
47 (Koven et al., 2013). Narrowing the uncertainty in estimated carbon emissions requires  
48 improvements in how Land Surface Models (LSMs) represent permafrost thermal and carbon  
49 dynamics.

Kevin Schaefer 12/3/2015 1:22 PM

**Deleted:** including carbon at depth below 3m

Kevin Schaefer 12/3/2015 1:22 PM

**Deleted:** Our rough estimates suggest that the total stock of the liable frozen carbon within top 3 meters could range between 500 to 600 GtC.

50 | The active layer in permafrost regions is the surficial soil layer overlying the permafrost,  
51 which undergoes seasonal freeze-thaw cycles. Active layer thickness (ALT) is the maximum  
52 depth of thaw at the end of summer. LSMs used to estimate emissions from thawing permafrost  
53 typically assume that the frozen carbon is located in the upper permafrost above 3 meters depth  
54 and below the maximum ALT (Koven et al., 2011; Schaefer et al., 2011; MacDougall et al.,  
55 2012). Thus, the simulated ALT determines the volume of permafrost in the top 3 meters of soil,  
56 and thus the initial amount of frozen carbon. Consequently, any biases in the simulated ALT  
57 | will influence the initial amount of frozen carbon, even if different models initialize the frozen  
58 carbon in the same way. Also, the same thermal biases that lead to deeper simulated active  
59 layers also lead to warmer soil temperatures, making the simulated permafrost more vulnerable  
60 to thaw and resulting in higher emissions estimates (Koven et al., 2013).

Kevin Schaefer 12/3/2015 1:23 PM

**Deleted:** could

61 | The surface organic layer (SOL) is the surface soil layer of nearly pure organic matter  
62 that exerts a huge influence on the thermodynamics of the active layer. The organic layer

68 thickness (OLT) usually varies between 5-30 cm, depending on a balance between the litter  
69 accumulation rate relative to the organic matter decomposition rate (Yi et al., 2009; Johnstone et  
70 al., 2010). A recent model intercomparison study shows that LSMs need more realistic surface  
71 processes such as an SOL and better representations of subsoil thermal dynamics (Ekici et al.,  
72 2014a). The low thermal conductivity of the SOL makes it an effective insulator decreasing the  
73 heat exchange between permafrost and the atmosphere (Rinke et al., 2008). The effect of the  
74 SOL has been well presented in several modeling studies. For example, Lawrence and Slater  
75 (2008) showed that soil organic matter affects the permafrost thermal state in the Community  
76 Land Model (CLM), and Jafarov et al., (2012) discussed the effect of the SOL in the regional  
77 modeling study for Alaska, United States. Recently, Chadburn et al., (2015a,b) incorporated the  
78 SOL in the Joint UK Land Environment Simulator (JULES) model to illustrate its influence on  
79 ALT and ground temperatures both at a site specific study in Siberia, Russia, and globally. In  
80 essence, the soil temperatures and ALT decrease as the OLT increases. Consequently, how (or  
81 if) LSMs represent the SOL in the simulated soil thermodynamics will simultaneously determine  
82 the initial amount of frozen permafrost carbon and the vulnerability of the simulated permafrost  
83 to thaw.

84 In this study we improved present day frozen carbon stocks in the Simple  
85 Biosphere/Carnegie-Ames-Stanford Approach (SiBCASA) model to reduce the bias of initial  
86 permafrost carbon stocks in simulations of future permafrost carbon release. To achieve this we  
87 introduced three improvements into the SiBCASA model: 1) improve the soil thermal dynamics  
88 and ALT, 2) improve soil carbon dynamics and build-up of carbon stocks in soil, and 3) initialize  
89 the older carbon using observed circumpolar soil carbon (Hugeluis et al., 2014).

Kevin Schaefer 12/3/2015 1:24 PM

**Deleted:** upper organic layer

Kevin Schaefer 12/3/2015 1:27 PM

**Deleted:** aimed to

Kevin Schaefer 12/3/2015 1:27 PM

**Deleted:** soil

Kevin Schaefer 12/3/2015 1:28 PM

**Deleted:** present day

Elchin Jafarov 11/16/2015 9:49 PM

**Deleted:** Here we describe a fully dynamic SOL to demonstrate the importance of coupling soil biogeochemistry and thermodynamics to improve the simulated permafrost temperature and ALT.

Elchin Jafarov 11/16/2015 9:50 PM

**Deleted:** w

Kevin Schaefer 12/3/2015 1:26 PM

**Deleted:** following

Kevin Schaefer 12/3/2015 1:26 PM

**Deleted:** firstly

Kevin Schaefer 12/3/2015 1:27 PM

**Deleted:** secondly

Kevin Schaefer 12/3/2015 1:27 PM

**Deleted:** finally

Kevin Schaefer 12/3/2015 1:28 PM

**Deleted:** current

Elchin Jafarov 11/16/2015 9:51 PM

**Deleted:** improved the Simple Biosphere/Carnegie-Ames-Stanford Approach (SiBCASA) model (Schaefer et al., 2011) by adding a dynamic SOL and limiting plant growth in frozen soils and demonstrated that these changes improve permafrost thermal and carbon dynamics in comparison. Then we used the modified model to evaluate current permafrost carbon stock

Elchin Jafarov 11/16/2015 9:57 PM

**Deleted:** under the steady state climate in the early 20<sup>th</sup> century.

115 **2. Methods**

116 We used the SiBCASA model (Schaefer et al., 2008) to evaluate current soil carbon stocks in  
117 permafrost affected soils. SiBCASA has fully integrated water, energy, and carbon cycles and  
118 computes surface energy and carbon fluxes at 10 minute time steps. SiBCASA predicts the  
119 moisture content, temperature, and carbon content of the canopy, canopy air space, and soil  
120 (Sellers et al., 1996a; Vidale and Stockli, 2005). To calculate plant photosynthesis, the model  
121 uses a modified Ball-Berry stomatal conductance model (Ball, 1998; Collatz et al., 1991)  
122 coupled to a C3 enzyme kinetic model (Farquhar et al., 1980) and a C4 photosynthesis model  
123 (Collatz et al., 1992). It predicts soil organic matter, surface litter, and live biomass (leaves,  
124 roots, and wood) in a system of 13 prognostic carbon pools as a function of soil depth (Schaefer  
125 et al., 2008). The model biogeochemistry does not account for disturbances, such as fire, and  
126 does not include a nitrogen cycle. SiBCASA separately calculates respiration losses due to  
127 microbial decay (heterotrophic respiration) and plant growth (autotrophic respiration).

128 SiBCASA uses a fully coupled soil temperature and hydrology model with explicit  
129 treatment of frozen soil water originally from the Community Climate System Model, Version  
130 2.0 (Bonan, 1996; Oleson et al., 2004). To improve simulated soil temperatures and permafrost  
131 dynamics, Schaefer et al. (2009) increased the total soil depth to 15 m and added the effects of  
132 soil organic matter on soil physical properties. Simulated snow density and depth, and thus  
133 thermal conductivity, significantly influence simulated permafrost dynamics, so Schaefer et al.  
134 (2009) added the effects of depth hoar and wind compaction on simulated snow density and  
135 depth. Recent model developments include [accounting for substrate availability in frozen soil](#)  
136 biogeochemistry (Schaefer and Jafarov, 2015).

137 We spun SiBCASA up to steady-state initial conditions using an input weather dataset

Kevin Schaefer 12/3/2015 1:30 PM

~~Deleted:~~ improved numerical scheme for

139 from the Climatic Research Unit National Center for Environmental Predictions (CRUNCEP)<sup>1</sup>  
140 (Wei et al, 2014) for the entire permafrost domain in the northern hemisphere (Brown et al.,  
141 1997). CRUNCEP is modeled weather data at 0.5x0.5 degree latitude and longitude resolution  
142 optimally consistent with a broad array of observations. The CRUNCEP dataset used in this  
143 study spans 110 years, from 1901 to 2010. We selected the first 30 years from the CRUNCEP  
144 dataset (1901 to 1931) and randomly distributed them over 900 years. To run our simulations we  
145 used JANUS High Performance Computing (HPC) Center at University of Colorado at Boulder.  
146 The 900-yr time span was chosen in order to make optimal use of the computational time, which  
147 allowed us to finish one spinup simulation on JANUS HPC without interruptions.

148

### 149 *2.1.Frozen carbon initialization*

150 We initialized the frozen carbon stocks using the Northern Circumpolar Soil Carbon Dataset  
151 version 2 (NCSCDv2) (Hugeluis et al., 2013). The NCSCDv2 includes soil carbon density maps  
152 in permafrost-affected soils available at several spatial resolutions ranging from 0.012° to 1°. The  
153 dataset consists of spatially extrapolated soil carbon data from more than 1700 soil core samples.  
154 This dataset has three main layers, each 1 meter in depth, distributed between ground surface and  
155 3 meter depth.

156 We placed the frozen carbon within the top three meters of simulated permafrost, ignoring  
157 deltaic and loess deposits that are known to extend well beyond 3 meters of depth (Hugeluis et  
158 al., 2014). The bottom of the permafrost carbon layer is fixed at 3 meters, while the top varies  
159 spatially depending on the simulated ALT during the spinup run. We initialized the permafrost  
160 carbon by assigning carbon from the NCSCDv2 to the frozen soil carbon pools below the

<sup>1</sup> [ftp://nacp.ornl.gov/synthesis/2009/frescati/temp/land\\_use\\_change/original/readme.htm](ftp://nacp.ornl.gov/synthesis/2009/frescati/temp/land_use_change/original/readme.htm)

Kevin Schaefer 12/3/2015 1:31 PM  
**Comment [2]:** The PCN did not publish the database, Hugeluis et al did

Kevin Schaefer 12/3/2015 1:31 PM  
**Deleted:** The Permafrost Carbon Network

Kevin Schaefer 12/3/2015 1:31 PM  
**Deleted:** published a revised

Kevin Schaefer 12/3/2015 1:33 PM  
**Formatted:** Indent: First line: 0"

Kevin Schaefer 12/3/2015 1:32 PM  
**Deleted:** with

Kevin Schaefer 12/3/2015 1:32 PM  
**Deleted:** changes in

Elchin Jafarov 11/19/2015 5:01 PM  
**Deleted:** Defining the permafrost table as the maximum ALT, we essentially assume that the soil above the permafrost table has thawed frequently enough over thousands of years to decay away all the old carbon.

Kevin Schaefer 12/3/2015 1:33 PM  
**Deleted:**

Elchin Jafarov 11/19/2015 5:01 PM  
**Deleted:** -

Kevin Schaefer 12/3/2015 1:33 PM  
**Deleted:** The current version of the model

Kevin Schaefer 12/3/2015 1:32 PM  
**Deleted:** s

174 | [maximum thaw depth. These frozen pools remained inactive until the layer thaws.](#)

175 | We initialized frozen carbon between the permafrost table and 3 meters depth using two  
176 | scenarios: 1) spatially uniform distribution of the frozen carbon throughout the permafrost  
177 | domain (Schaefer et al., 2011), and 2) observed distribution of the frozen carbon according to the  
178 | NCSCDv2. It is important to know the “stable” depth of the active layer before initializing  
179 | frozen carbon. We run the model for several years in order to calculate ALT, and then initialized  
180 | frozen carbon below the maximum calculated ALT. The frozen carbon was initialized only once  
181 | during the first equilibrium run cycle. For the next equilibrium run we used the previously  
182 | calculated permafrost carbon. We defined an equilibrium point when changes in overall  
183 | permafrost carbon were negligible or almost zero.

184 | The total initial frozen carbon in each soil layer between the permafrost table and 3  
185 | meters is

$$186 | C_{fr}^i = \rho_c \Delta z_i, \quad (1)$$

187 | where  $C_{fr}^i$  is the total permafrost carbon within the  $i^{\text{th}}$  soil layer,  $\rho_c$  is the permafrost carbon  
188 | density, and  $\Delta z_i$  is the thickness of the  $i^{\text{th}}$  soil layer in the model. For the uniform permafrost  
189 | carbon distribution,  $\rho_c = 21 \text{ kg C m}^{-3}$  and assumed to be spatially and vertically uniform  
190 | (Schaefer et al., 2011). For the observed distribution from the NCSCDv2,  $\rho_c$  varies both with  
191 | location and depth (Hugeluis et al., 2013).

192 | The [permafrost](#) carbon in each layer is divided into three [soil carbon](#) pools as follows:

$$193 | \begin{aligned} C_{slow}^i &= 0.8C_{fr}^i \\ C_{met}^i &= 0.2f_{root2met}C_{fr}^i \\ C_{str}^i &= 0.2f_{root2str}C_{fr}^i, \end{aligned} \quad (2)$$

194 | where  $f_{root2met}$  and  $f_{root2str}$  are the simulated fractions of root pool losses to the soil metabolic

Kevin Schaefer 12/3/2015 1:34 PM

Deleted:

196 and structural pools respectively (Schaefer et al., 2008). The nominal turnover time is 5 years  
197 for the slow pool, 76 days for the structural pool, and 20 days for the metabolic pool. Schaefer et  
198 al. (2011) has a 5% loss to the metabolic pool and a 15% loss to the structural pool based on  
199 observed values in Dutta et al. (2006). The simulated fractions are actually 5.6% to the  
200 metabolic pool and 14.4% to the structural pool. We found it encouraging that the numbers  
201 calculated with the SiBCASA metabolic fractions resulted in numbers that are close to the  
202 observed values in Dutta et al. (2006).

203

## 204 *2.2. Dynamic SOL*

205 We modified SiBCASA to include a dynamic SOL by incorporating the vertical redistribution of  
206 organic material associated with soil accumulation. SiBCASA calculates the soil physical  
207 properties as a weighted average of those for organic matter, mineral soil, ice and water  
208 (Schaefer et al., 2009). The physical properties include soil porosity, hydraulic conductivity,  
209 heat capacity, thermal conductivity, and matric potential. The model calculates the organic  
210 fraction used in the weighted mean as the ratio of simulated carbon density to the density of pure  
211 organic matter. SiBCASA does not account for the compression of organic matter. Since the  
212 prognostic soil carbon pools vary with depth and time, the organic fraction and the physical  
213 properties all vary with time and depth. We only summarized these calculations here since the  
214 calculations are covered in detail in Schaefer et al. (2009).

215 The previous version of the model distributed fine and coarse root growth vertically within the  
216 soil column based on observed root distributions. As the roots die, carbon is transferred to the  
217 soil carbon pools for that layer. Thus, the maximum rooting depth determined the maximum  
218 depth of 'current' or 'active' carbon in the model. Of course, if the maximum rooting depth fell

Kevin Schaefer 12/3/2015 1:39 PM

**Comment [3]:** The paragraph formatting is inconsistent. Some are indented and some are not.

Kevin Schaefer 12/3/2015 1:36 PM

**Deleted:** of

Kevin Schaefer 12/3/2015 1:37 PM

**Deleted:** Each model layer has a complete set of prognostic soil carbon pools.

222 | below the permafrost table, the model would accumulate permafrost carbon, which remains  
223 | inactive until the layer thaws. As live, above-ground biomass in the model dies, carbon is  
224 | transferred into the first layer as litter. Without the vertical redistribution we describe here to  
225 | create a surface organic layer, the top layer of the model tended to accumulate carbon in excess  
226 | of that expected for pure organic matter.

Kevin Schaefer 12/3/2015 1:38 PM

**Deleted:** . The current version of the model initializes the permafrost carbon by assigning carbon to the soil carbon pools below the maximum thaw depth. These frozen pools

Kevin Schaefer 12/3/2015 1:38 PM

**Deleted:** remained

227 | To allow vertical movement and build up a SOL, we placed a maximum limit on the amount of  
228 | organic material that each soil layer can hold. When the simulated carbon content exceeds this  
229 | threshold, the excess carbon is transferred to the layer below. This is a simplified version of the  
230 | Koven et al., (2009) carbon diffusion model, which accounts for all sedimentation and  
231 | cryoturbation processes, because we wanted to limit our model only to the buildup of a SOL.

Kevin Schaefer 12/3/2015 1:39 PM

**Deleted:** while

232 | We calculate the maximum allowed carbon content per soil layer,  $C_{max}$ , as

$$233 \quad C_{max} = \rho_{max} \Delta z \frac{1000}{MW_C}, \quad (3)$$

234 | where  $\rho_{max}$  is the density of pure organic matter or peat,  $\Delta z$  is the soil layer thickness (m),  $MW_C$   
235 | is the molecular weight of carbon (12 g mol<sup>-1</sup>), and the factor of 10<sup>3</sup> converts from grams to  
236 | kilograms. Based on observations of bulk densities of peat, we assume  $\rho_{max}$  is 140 kg m<sup>-3</sup>  
237 | (Price et al., 2005). The  $MW_C$  term converts the expression into mol C m<sup>-2</sup>, the SiBCASA  
238 | internal units for carbon. The simulated organic soil fraction per soil layer,  $f_{org}$ , is defined as

$$239 \quad f_{org} = \frac{C}{C_{max}}, \quad (4)$$

240 | where  $C$  is the carbon content per soil layer (mol m<sup>-2</sup>). To convert to carbon we assume that the  
241 | fraction of organic matter is 0.5, which means that half of the organic matter by mass is carbon.  
242 | The original formulation allowed  $f_{org}$  to exceed 1.0 such that the excess organic material was



249 essentially ‘compressed’ into the top soil layer, resulting in a 2-cm simulated SOL. We place an  
250 upper limit of 0.95 on  $f_{org}$  and transfer the excess carbon to the layer below. The OLT is  
251 defined as the bottom of the lowest soil layer where  $f_{org}$  is 0.95.

252

253

### 254 2.3. Coupling growth to thaw depth

255 We coupled simulated gross primary productivity (GPP), plant phenology, and root growth to simulated  
256 thaw depth as a function of time. The model assumes root growth decreases exponentially with depth  
257 based on observed vertical root distributions (Jackson et al., 1996; Schaefer et al., 2008). The maximum  
258 rooting depth for completely thawed soil is defined as the soil depth corresponding to 99% of the  
259 observed vertical root distribution or 1.1 m for the tundra and boreal forest biomes. In real life, growing  
260 roots cannot penetrate frozen soil (Tryon and Chapin 1983, Van Cleve et al., 1983), so we restricted  
261 simulated root growth to occur only within the thawed portion of the active layer. The date of snowmelt  
262 determines the start date of the growing season and the start of active layer thawing (Grøndahl et al. 2007;  
263 Wipf and Rixen 2010). Since fine root and leaf growth are coupled (Schaefer et al., 2008), constraining  
264 root growth to thawed soil also constrains spring leafout to occur after the active layer starts thawing. In  
265 real life plants cannot photosynthesize without liquid water in the soil, so we scaled simulated GPP based  
266 on the fraction of thawed roots in the root zone.

267 We restricted simulated root growth to occur only in thawed soil layers. In SiBCASA, leaf  
268 growth is linked to fine root growth (Schaefer et al., 2008), so this also delays spring leafout until  
269 the soil begins to thaw. We first calculated the fraction of thawed roots within the root zone  
270 defined by:

Kevin Schaefer 12/3/2015 5:59 PM  
**Deleted:** Root growth and soil thermal freezing factor

Elchin Jafarov 12/19/2015 5:45 PM  
**Deleted:** SiBCASA

Elchin Jafarov 12/19/2015 5:45 PM  
**Deleted:** ( $D_{root}$ )

Elchin Jafarov 12/19/2015 5:48 PM  
**Deleted:**  $D_{root}$

276 
$$R_{th} = \sum_{i=1}^{n_{root}} R_{fi} (1 - F_{ice_i}), \quad (6)$$

277 where  $R_{th}$  is the fraction of total roots that are thawed,  $n_{root}$  is the soil layer corresponding to  
 278 root depth,  $R_{fi}$  is the reference root fraction for the  $i^{th}$  soil layer based on observed root  
 279 distributions, and  $F_{ice_i}$  is the ice fraction calculated from the simulated ice content for the  $i^{th}$  soil  
 280 layer. When  $R_{th}$  equals one, the entire root zone is thawed and when  $R_{th}$  is zero, the entire root  
 281 zone is frozen. We assume evenly distributed liquid water in each layer such that  $F_{ice}$  equals the  
 282 frozen soil fraction. We then calculated  $R_{eff_i}$  the effective root fraction for the  $i^{th}$  soil layer,

283 
$$R_{eff_i} = R_{fi} (1 - F_{ice_i}) / R_{th}. \quad (7)$$

284 We then use  $R_{eff_i}$  to distribute new fine and coarse root growth within the soil column. When  
 285  $R_{eff_i}$  equals zero, the soil layer is frozen with no root growth. Dividing by  $R_{th}$  ensures  $R_{eff_i}$   
 286 sums to one within the soil column to conserve mass. This formulation makes the effective  
 287 maximum rooting depth, equal to the thaw depth.

288 To couple GPP to thaw depth, we treated the reference root zone distribution for completely  
 289 thawed soil as the maximum root growth capacity defining the maximum potential GPP. When  
 290  $R_{th} < 1$ , the root zone is partially frozen and GPP is less than its full potential. We defined a GPP  
 291 scaling factor,  $S_{soilfrz}$ , as

292 
$$S_{soilfrz} = \begin{cases} R_{th} & \text{for } R_{th} \geq 0.01 \\ 0 & \text{for } R_{th} < 0.01 \end{cases} \quad (8)$$

293 This assumes that at least 1% of the roots must be thawed for GPP to occur, corresponding to  
 294 about ~1 cm of thawed soil.  $S_{soilfrz}$  is applied along with the drought stress and temperature

- Elchin Jafarov 12/19/2015 5:48 PM  
Deleted: nr
- Elchin Jafarov 12/19/2015 5:48 PM
- Elchin Jafarov 12/19/2015 5:49 PM  
Deleted:  $R_{fi}$
- Elchin Jafarov 12/19/2015 5:49 PM  
Deleted:  $n_{root}$
- Elchin Jafarov 12/19/2015 5:49 PM  
Deleted:  $D_{root}$
- Elchin Jafarov 12/19/2015 5:41 PM  
Deleted:  $R_{fi}$
- Elchin Jafarov 12/19/2015 5:41 PM  
Deleted:  $F_{ice_i}$
- Elchin Jafarov 12/19/2015 5:40 PM  
Deleted:  $R_{eff}$
- Kevin Schaefer 12/3/2015 6:04 PM  
Formatted: Font:Not Italic, Not Superscript/ Subscript
- Elchin Jafarov 12/19/2015 5:39 PM  
Deleted:  $eff_i$
- Elchin Jafarov 12/19/2015 5:40 PM  
Deleted:  $f_i$
- Elchin Jafarov 12/19/2015 5:39 PM  
Deleted:  $ic$
- Elchin Jafarov 12/19/2015 5:40 PM  
Deleted:  $ei$
- Elchin Jafarov 12/19/2015 5:40 PM  
Deleted:  $R_{eff_i}$
- Elchin Jafarov 12/19/2015 5:40 PM  
Deleted:  $R_{eff}$
- Elchin Jafarov 12/19/2015 5:40 PM  
Deleted:  $R_{eff}$
- Elchin Jafarov 12/19/2015 5:41 PM  
Deleted:  $D_{rooteffs}$

311 [scaling factors to constrain photosynthesis \(Schaefer et al., 2008\)](#). SiBCASA assumes that the  
312 [factors that control GPP also control wood and leaf growth, so we also included  \$S\_{soilfr}\$  as a new](#)  
313 [scaling factor in addition to the drought stress and temperature scaling factors that control wood](#)  
314 [and leaf growth.](#)

315 ↓

### 316 3. Results

317 The dynamic SOL decreased the simulated ALT on average 50% across the domain and allowed  
318 the model to simulate permafrost in discontinuous zones where it could not before (Figure 1).  
319 The area of near surface permafrost simulated with the current version of the model equals to  
320 13.5 mil km<sup>2</sup> which is almost 38% greater than without the dynamic SOL (Schaefer et al., 2011).  
321 This area is closer to the [observed area](#) from the International Permafrost Association: 16.2 mil  
322 km<sup>2</sup> (Brown et al., 1997). Simulated ALT less than 2 m covers about 92% of the area in the new  
323 simulations (Figure 1B) in comparison to 66% of the area in the Schaefer et al. (2011)  
324 simulations (Figure 1A). The previous version of SiBCASA could not simulate permafrost in  
325 many parts of the discontinuous zone with relatively warm climate. Adding the dynamic SOL  
326 essentially decreased the thermal conductivity of the surface soil [allowing](#) SiBCASA to simulate  
327 permafrost where the mean annual air temperatures (MAAT) are close to 0 °C.

328 To illustrate the improvement of the simulated ALT with respect to the observed data, we  
329 compared simulated ALT with measured values from Circumpolar Active Layer Monitoring  
330 (CALM) stations. The CALM network is a part of the Global Terrestrial Network for Permafrost  
331 (GTN-P) (Burgess et al., 2000). The monitoring network measures ALT either using a  
332 mechanical probe or a vertical array of temperature sensors (Brown et al., 2000; Shiklomanov et  
333 al., 2010). After matching up the CALM coordinates with the coordinates of previously

Kevin Schaefer 12/3/2015 1:44 PM

**Comment [4]:** You need to insert the reference

Kevin Schaefer 12/3/2015 5:59 PM

**Deleted:** Fine roots supply nutrients and water for photosynthesis, so essentially the leaves and roots together define the photosynthetic capacity of the plant. Plants have optimized carbon allocation to grow only enough fine roots to properly supply the leaves with the correct amount of water and nutrients to support photosynthesis. So, as plants grow new leaves, they also grow new fine roots to supply them with nutrients and water. Linking root growth to leaf growth is a convenient and simple way to represent this coupling in SiBCASA. ... [1]

Kevin Schaefer 12/3/2015 1:48 PM

**Deleted:** observation

Kevin Schaefer 12/3/2015 1:49 PM

**Deleted:** which is about

Kevin Schaefer 12/3/2015 1:49 PM

**Deleted:** to

349 simulated ALT (Schaefer et al., 2011), we excluded sites with no measurements or ALT greater  
350 than 3m depth, ending up with 76 CALM stations. Figure 2 shows simulated vs. observed ALT  
351 for the 76 CALM sites. The current simulations have a higher resolution than Schaefer et al.  
352 (2011) simulations, which allowed us to reach a higher order of heterogeneity between measured  
353 and simulated ALTs. The Pearson's correlation coefficient,  $R$ , is negative and not significant for  
354 the Schaefer et al. (2011) simulations (Figure 2A), but is positive and statistically significant for  
355 the current simulations assuming  $p < 0.05$  (Figure 2B). The dynamic SOL greatly improves the  
356 simulated ALT, but SiBCASA still tends to overestimate ALT.

357 Figure 3 illustrates the effect of the frozen soil restrictions on phenology and GPP at a  
358 single point in central Siberia. Before applying a frozen soil restriction, SiBCASA maintained  
359 fine roots even in winter, resulting in root growth all year with a peak in spring corresponding to  
360 simulated leafout (Figure 3A). Simulated GPP was restricted by liquid water availability and  
361 was closely tied to thawing of the active layer, resulting in a lag as high as 60 days between  
362 leafout and start of GPP in spring. Restricting growth and GPP to when the soil is thawed  
363 essentially synchronizes all phenological events to occur at the same time (Figure 3B).

364 Restricting growth and GPP to when the soil is thawed delayed the onset of plant  
365 photosynthesis in spring in permafrost-affected regions. Introduction of the thawed root fraction  
366 in the model reduced GPP primarily in early spring. To illustrate the difference between  
367 unconstrained and restricted root growth (Figure 3), we ran the model for ten years for both  
368 cases. The difference between unconstrained and restricted root growth resulted in an overall  
369 ~9% reduction in GPP for the entire permafrost domain, nearly all of which occurred in spring.

370 The simplified scheme of the soil carbon dynamics improves permafrost resilience, but  
371 does not fully reproduce observed carbon distribution with depth (Harden et al., 2012). To

Elchin Jafarov 11/19/2015 5:15 PM

**Deleted:** In the previous version without a dynamic SOL the ALT was generally deep in forest biomes, but in the new version there is a thick SOL (due to high GPP), which leads to a shallower ALT. Without restricting root growth within only thawed part of the soil the shallower ALT feedback leads to a significant amount of root growth in the permafrost itself, which puts carbon directly into the permafrost stores. This is unrealistic since growing roots cannot penetrate frozen soil, so the frozen soil restrictions on GPP and root growth together eliminate this problem.

Elchin Jafarov 11/19/2015 5:16 PM

**Deleted:** cases

Elchin Jafarov 11/19/2015 3:25 PM

**Deleted:** (Figure 4) indicates

Kevin Schaefer 12/3/2015 2:13 PM

**Comment [5]:** This sentence does not belong here. It appears to be unrelated to the rest of the paragraph.

386 illustrate soil carbon distribution with depth we selected three representative areas: a continuous  
387 permafrost area corresponding to tundra type biome above the Arctic circle, an area in the  
388 boundary of continuous and discontinuous permafrost corresponding to the boreal forest biome,  
389 and an area near the south border of the discontinuous permafrost corresponding to poorly  
390 vegetated-rocky areas. We calculated mean and standard deviation of the carbon density  
391 distribution with depth for 200 grid points around each of the three selected locations. Simulated  
392 typical carbon densities from [the](#) selected locations are shown on Figure 4. All profiles shown on  
393 Figure 4 show a similar pattern: a 20-30 cm SOL with reduced carbon content at the bottom of  
394 the active layer.

395 [The decrease in ALT resulting from a dynamic SOL increases the volume of permafrost](#)  
396 in the top 3 meters of soil, greatly increasing the initial amount of frozen permafrost carbon in  
397 the simulations. Schaefer et al. (2011) without the dynamic SOL assumed a uniform permafrost  
398 carbon density of  $21 \text{ kg} \cdot \text{C} \cdot \text{m}^{-3}$ , resulting in a total of 313 Gt of permafrost carbon at the start  
399 of their transient run (Figure 5A). To compare with the Schaefer et al. [2011] results, we  
400 initialized the permafrost carbon using the same assumed uniform carbon density and ran  
401 SiBCASA to steady state initial conditions (Figure 5B). Assuming the same uniform carbon  
402 density, the current version with the dynamic SOL results in a total of ~680Gt C compared to  
403 313 GtC in Schaefer et al. (2011). The dynamic SOL effectively doubled the volume of  
404 permafrost in the top three meters of soil and the amount of simulated frozen carbon.

405 [Initializing SiBCASA with the observed spatial distribution of permafrost carbon from](#)  
406 [the NCSCDv2 resulted in ~560 GtC of carbon stored in permafrost after spinup. This](#) does not  
407 mean that after the spinup simulated permafrost carbon stocks exactly matched the NCSDC data.  
408 During spinup, ALT varies with time, introducing carbon movement from frozen to thawed

Elchin Jafarov 11/19/2015 7:54 PM

Deleted: 5

Elchin Jafarov 11/19/2015 7:54 PM

Deleted: 5

Elchin Jafarov 11/19/2015 5:17 PM

Deleted:

Kevin Schaefer 12/3/2015 2:12 PM

**Comment [6]:** We should not delete this since it explains the carbon depletion at the permafrost table

Elchin Jafarov 11/19/2015 5:17 PM

**Deleted:** In contrast, the observed vertical carbon profiles show fairly uniform carbon density with depth throughout the active layer and into the permafrost Harden et al., (2012). SiBCASA lacks the cryoturbation processes such as cryotic mixing that would redistribute carbon within the active layer. As a result, the carbon at the bottom of the active layer decayed and respired away during spinup.

Elchin Jafarov 11/19/2015 5:18 PM

Deleted: -

Elchin Jafarov 11/19/2015 7:55 PM

Deleted: 6

Elchin Jafarov 11/19/2015 7:55 PM

Deleted: 6

Kevin Schaefer 12/3/2015 1:56 PM

Moved (insertion) [3]

Elchin Jafarov 11/19/2015 5:24 PM

**Formatted:** Normal, Left, Indent: First line: 0.5", Space Before: 0 pt, After: 12 pt, No widow/orphan control, Don't adjust space between Latin and Asian text, Don't adjust space between Asian text and numbers

Kevin Schaefer 12/3/2015 1:56 PM

**Deleted:** Prescribing permafrost carbon according to the NCSDC dataset allowed us to better match with the observed pattern in the soil carbon and overall amount of the frozen carbon.

Elchin Jafarov 11/19/2015 5:20 PM

Deleted: However, it is

428 pools. In discontinuous zones, if the model simulated permafrost, it tended to produce a deeper  
429 ALT and thus less permafrost carbon than the NCSCD. The major difference between uniform  
430 frozen carbon initialization (Fig 6A) and initialization using the NCSCD (Fig 6B) is that  
431 SiBCASA simulated permafrost in more places. However, the NCSCD map (Fig 6B) shows that  
432 not all permafrost regions contain a uniform amount of frozen carbon. Therefore simulating  
433 'correct' ALT is important and should improve the overall permafrost carbon storage.

#### 435 4. Discussion

436 In the original SiBCASA formulation without a dynamic SOL, near surface air temperature  
437 (NSAT) controlled leaf and fine root growth: when the air temperature exceeded 0°C, leaves and  
438 roots started to grow. However, both air temperature and the availability of liquid water in the  
439 active layer controlled simulated GPP such that photosynthesis would not start until the active  
440 layer began to thaw. As a result, the simulated leafout and new root growth occurred as many as  
441 60 days before the start of photosynthesis in spring. In addition, root depth often exceeded the  
442 simulated thaw depth, resulting in root growth in frozen soil. This was a minor problem in the  
443 original SiBCASA formulation, which simulated relatively deep active layers. However, once  
444 we implemented a dynamic SOL and reduced the ALT, the simulated roots grew directly into the  
445 permafrost and froze. The frozen roots died, but never decayed, resulting in an unrealistic  
446 buildup of simulated frozen carbon in the upper layers of permafrost. Essentially, implementing  
447 a dynamic SOL also requires coupling of GPP, plant phenology, and root growth to simulated  
448 thaw depth.

449 SiBCASA underestimated the SOC in the Eastern Canada and Western Siberia, and

Elchin Jafarov 11/19/2015 7:56 PM  
**Deleted:** 7

Kevin Schaefer 12/3/2015 1:55 PM  
**Deleted:** according to

Elchin Jafarov 11/19/2015 7:56 PM  
**Deleted:** 7

Elchin Jafarov 11/19/2015 7:56 PM  
**Deleted:** 7

Kevin Schaefer 12/3/2015 1:55 PM  
**Deleted:** frozen soil contains

Kevin Schaefer 12/3/2015 1:56 PM  
**Moved up [3]:** Initializing SiBCASA with the observed spatial distribution of permafrost carbon from the NCSCDv2 resulted in ~560 GtC of carbon stored in permafrost after spinup.

Elchin Jafarov 11/19/2015 5:25 PM  
**Moved down [1]:** SiBCASA underestimated the SOC in the Eastern Canada and Western Siberia, and overestimated SOC in Central Siberia (Figure 7A and B). Failure to simulate soil carbon in southeast Canada and southwest Siberia (Figure 7C) could be attributed to deep active layer thickness. The overestimation of SOC in Central Siberia is a result of coupling between GPP and ALT. The overall amount of soil frozen carbon is less than that calculated assuming uniform frozen carbon distribution. It is important to note that the SOL, ALT, and the permafrost thickness are the same for both cases (Figure 7A and B). This is due to the fact that in both cases soil carbon is added in the permafrost layer below the active layer. Consequently, the amount of soil carbon in the active layer stays does not change between simulations and has the same thermal and carbon dynamics, and thus ALT. The smaller permafrost carbon stock simulated for the non-uniform case is mainly due to the fact that we did not initialize frozen carbon in regions where according to the NCSCDv2 it is not present, such as the Brooks Range in Alaska.

Elchin Jafarov 11/19/2015 5:25 PM  
**Deleted:** .

Elchin Jafarov 11/19/2015 5:25 PM  
**Formatted:** Font:(Default) Times New Roman, 12 pt

Elchin Jafarov 11/19/2015 5:25 PM  
**Formatted:** Font:(Default) Times New

Kevin Schaefer 12/3/2015 2:15 PM  
**Comment [7]:** The flow in the discussion section is disjointed. Several paragraphs contain a m... [2]

Elchin Jafarov 12/19/2015 5:43 PM  
**Deleted:**  $D_{root}$

Kevin Schaefer 12/3/2015 1:59 PM  
**Comment [8]:** This paragraph does not make sense. It seems to cover two different topics.

Elchin Jafarov 11/19/2015 5:25 PM  
**Moved (insertion) [1]**

Elchin Jafarov 11/19/2015 5:25 PM  
**Formatted:** Indent: First line: 0"

484 overestimated SOC in Central Siberia (Figure 6A and B). Failure to simulate soil carbon in  
 485 southeast Canada and southwest Siberia (Figure 6C) is attributed to deep active layer thickness.  
 486 The overestimation of SOC in Central Siberia is a result of coupling between GPP and ALT.  
 487 The overall amount of permafrost carbon is less than that calculated assuming uniform frozen  
 488 carbon distribution. It is important to note that the SOL, ALT, and the permafrost thickness are  
 489 the same for both cases (Figure 6A and B). This is due to the fact that in both cases soil carbon  
 490 is added in the permafrost layer below the active layer. Consequently, the amount of soil carbon  
 491 in the active layer stays does not change between simulations and has the same thermal and  
 492 carbon dynamics, and thus ALT. The smaller permafrost carbon stock simulated for the non-  
 493 uniform case is mainly due to the fact that we did not initialize frozen carbon in regions where  
 494 according to the NCSCDv2 it is not present, such as the Brooks Range in Alaska.

495       The dynamic SOL insulates ALT from air temperature, allowing SiBCASA to simulate  
 496 permafrost in many discontinuous permafrost regions where it could not before consistent with  
 497 previous results (Lawrence and Slater, 2008; Yi et al., 2009; Ekici et al., 2014b; Chadburn et al.,  
 498 2015a,b), when changes in thermal properties associated with the presence of soil organic matter  
 499 cooled the ground. In addition, our work confirms findings by Koven et al., (2009) showing that  
 500 including SOL dynamics into the model improves agreement with the observed permafrost  
 501 carbon stocks. However, to better simulate known permafrost distribution in the discontinuous  
 502 permafrost zone it is important to know the exact OLT. Unfortunately, in situ measurements of  
 503 OLT are scarce and essentially lacking in most areas of continuous and discontinuous  
 504 permafrost.

505 The simulated ALT is most influenced by NSAT and soil wetness fraction (SWF), with a slightly  
 506 smaller influence by down-welling long-wave radiation (DLWR), and nonlinearly influenced by

- Elchin Jafarov 11/19/2015 7:57 PM  
**Deleted:** 7
- Elchin Jafarov 11/19/2015 7:57 PM  
**Deleted:** 7
- Elchin Jafarov 12/19/2015 5:43 PM  
**Deleted:** could be
- Kevin Schaefer 12/3/2015 1:59 PM  
**Comment [9]:** use the same term everywhere
- Kevin Schaefer 12/3/2015 1:57 PM  
**Deleted:** soil frozen
- Elchin Jafarov 11/19/2015 7:57 PM  
**Deleted:** 7
- Kevin Schaefer 12/3/2015 1:59 PM  
**Deleted:** .
- Elchin Jafarov 11/19/2015 5:34 PM  
**Formatted:** Indent: First line: 0.5"
- Kevin Schaefer 12/3/2015 6:56 PM  
**Deleted:** . This result complements similar findings by
- Kevin Schaefer 12/3/2015 6:57 PM  
**Deleted:** Lawrence and Slater (2008), Yi et al., (2009), Ekici et al., (2014b), and Chadburn et al., (2015a,b),
- Kevin Schaefer 12/3/2015 6:58 PM  
**Deleted:** inclusion of
- Kevin Schaefer 12/3/2015 6:58 PM  
**Deleted:** the surface carbon layer
- Kevin Schaefer 12/3/2015 6:58 PM  
**Deleted:** leads to an improved
- Kevin Schaefer 12/3/2015 6:58 PM  
**Deleted:** estimated
- Kevin Schaefer 12/3/2015 6:58 PM  
**Deleted:** in permafrost-affected soils
- Kevin Schaefer 12/3/2015 7:00 PM  
**Deleted:** thickness of the upper soil organic layer
- Kevin Schaefer 12/3/2015 2:10 PM  
**Comment [10]:** I am not sure this is the reason. I see no references on the actual OLT to back this up. Also, this sentence does not relate to the rest of the paragraph.
- Kevin Schaefer 12/3/2015 7:00 PM  
**Deleted:** Our setup does not include thick organic layer along the southeastern boundaries of the permafrost domain in Canada as well as southwestern part of Russia, which did not allow the model to simulate permafrost in those regions. In
- Elchin Jafarov 11/19/2015 5:34 PM  
**Deleted:** southeastern Canada and southwestern Siberia, SiBCASA simulates ALT up to 3 meter, and therefore almost no frozen carbon. For example, observed mean annual ground temperatures within southeast Canada region ranges from below to above 0 °C (Smith, and Burgess, 2000), which suggests that the actual permafrost distribution and associated ALT in these regions would be highly heterogeneous. Models like SiBCASA cannot ... [3]

549 snow depth (SD) (Figure 8). To show the influence of the NSAT we averaged two early fall  
 550 months over 10 years. The areas with deep simulated ALT correspond to annual NSAT > 1° C  
 551 in southwest Siberia and NSAT > 5° C in the southeast Canada with a statistically significant  
 552 correlation of 0.62. DLWR showed a similar, but slightly weaker relationship with ALT, with  
 553 deeper ALT in southeast Canada and southwest Siberia and statistically significant correlation of  
 554 0.45. Our results show no correlation between SD and ALT, but the effects of snow on ALT are  
 555 less obvious and depend on different physical processes, such as wind, snow metamorphism, and  
 556 depth hoar formation (Ekici et al., 2014; Jafarov et al., 2014). Zhang (2005) indicates that SND  
 557 less than 50cm have the greatest impact on soil temperatures. Figure 8C shows maximum  
 558 simulated snow depth calculated over the last 10 years of the steady state run. We also observe  
 559 high SWF in southwest Siberia and southeast Canada where SiBCASA simulates deep ALT with  
 560 a statistically significant correlation of 0.68, suggesting wet soils modulate the insulating effects  
 561 of the SOL (Lawrence and Slater, 2008).

562 The dynamic SOL and rooting depth strengthens the feedback between GPP and ALT  
 563 (Koven et al., 2009). Higher GPP produces greater litter fall, which increases the input soil  
 564 carbon at the surface and results in a thicker SOL. The dynamic SOL changes the properties of  
 565 the near surface soil, resulting in a shallower ALT and cooler soil temperatures. The dynamic  
 566 rooting depth accounts for a shallower ALT and modulates GPP accordingly. The cooler soil  
 567 temperatures slow microbial decay and increase the carbon accumulation rate, which in turn  
 568 increases the SOL and reduces ALT further. Eventually, this feedback results in the  
 569 development of a peat bog. The changes we describe here indicate that SiBCASA can simulate  
 570 the dynamics of peat bog development, but the model does not yet include a dynamic vegetation  
 571 model to account for conversions between biome types, such as boreal forest to peat bog.

Elchin Jafarov 12/19/2015 5:52 PM  
**Deleted:** , and a low influence by snow depth (SD)

Elchin Jafarov 12/19/2015 5:58 PM  
**Deleted:** Sturm et al., 1997

Elchin Jafarov 12/19/2015 5:59 PM  
**Deleted:** The influence of SD rapidly decreases for SD > 50 cm (Zhang, 2005; Ekici et al., 2014).

Elchin Jafarov 12/19/2015 6:01 PM  
**Deleted:** see

Kevin Schaefer 12/3/2015 2:13 PM  
**Comment [11]:** This sentence does not belong here. It appears to be unrelated to the rest of the paragraph.

Elchin Jafarov 12/19/2015 6:02 PM  
**Deleted:** To address the effect of different environmental factors we correlated ALT with near surface air temperature (NSAT), down-welling long-wave radiation (DLWR), snow depth (SND), and soil wetness fraction (SWF). The NSAT has a significant effect on the ALT (Camill 2005, Gallagher et al., 2011). To show this influence, we averaged NSAT in early fall, for two months September and October over 10 years (Figure 8A). The areas with deep ALT (Figure 1B) fall into the regions where NSATs are greater than one degree centigrade and greater than 5 °C in the south-east Canada. Figure 9A shows the correlation between NSAT and ALT, which indicates clear relation between NSAT and ALT. Including dynamic SOL in the model allows us to allows us to study the interaction of plant dynamics and soil thermodynamics. In addition it allows us to study other processes in the future, such as

Elchin Jafarov 11/19/2015 5:29 PM  
**Formatted:** Justified, Space After: 10 pt, Widow/Orphan control, Adjust space between Latin and Asian text, Adjust space between Asian text and numbers

Elchin Jafarov 11/19/2015 5:29 PM  
**Moved (insertion) [2]**

Kevin Schaefer 12/3/2015 2:13 PM  
**Deleted:** The simplified scheme of the soil carbon dynamics improves permafrost resilience, but does not fully reproduce observed carbon distribution with depth (Harden et al., 2012).

Elchin Jafarov 11/19/2015 5:29 PM  
**Deleted:** .



601 This work does not address the fire impacts on soil thermodynamics and recovery from  
 602 fire, both of which are strongly influenced by the changes in the SOL (Jafarov et al., 2013).  
 603 Studies show that wildfires and climate change could substantially alter soil carbon storage  
 604 (Yuan et al., 2012; Yi et al., 2010). In the current version of the model the topsoil carbon stays  
 605 in the system and provides resilience to permafrost. However, in reality, upper SOL could be  
 606 removed by fire, which would alter soil thermal properties and perturb permafrost carbon  
 607 stability.

609 **5. Conclusion**

610 This work shows the dynamic organic layer directly improves the distribution of carbon in soil,  
 611 as well as indirectly through the improved ALT. Initialization of the carbon according to the  
 612 NCSCD map allowed us to better match with the observed carbon distribution. Restriction of the  
 613 root growth within the thawed layer prevented soil from artificial accumulation of permafrost  
 614 carbon. As a result of the model developments we improved the distribution of permafrost  
 615 carbon storage by 259 GtC.  
 616 Most of the LSMs calculate soil properties based on prognostic soil carbon and soil texture from  
 617 Harmonized World Soil Carbon Database (HWSD). We found that HWSD does not include thermal  
 618 properties of peat lands, which resulted in inaccurate modeling of the ALT at the south boundaries of the  
 619 permafrost domain in Canada and Russia. We suggest to modified the HWSD to address low thermal  
 620 conductivities of the peat lands.

621 

- Elchin Jafarov 11/19/2015 5:36 PM  
**Deleted:** Including dynamic SOL in the mo ... [4]
- Elchin Jafarov 11/19/2015 5:38 PM  
**Deleted:** For example,
- Elchin Jafarov 11/19/2015 5:38 PM  
**Deleted:** (
- Elchin Jafarov 11/19/2015 5:38 PM  
**Deleted:** ) evaluated the role of wildfire in ... [5]
- Elchin Jafarov 11/19/2015 5:38 PM  
**Deleted:** , showing wildfires and climate ch ... [6]
- Elchin Jafarov 11/19/2015 5:38 PM  
**Deleted:** The current
- Elchin Jafarov 11/19/2015 5:38 PM  
**Deleted:** does not include the effects of fir ... [7]
- Elchin Jafarov 12/19/2015 6:10 PM  
**Formatted** ... [8]
- Elchin Jafarov 11/19/2015 8:04 PM  
**Formatted** ... [9]
- Elchin Jafarov 11/19/2015 8:04 PM  
**Formatted** ... [10]
- Kevin Schaefer 12/3/2015 2:15 PM  
**Deleted:** thaw depth
- Kevin Schaefer 12/3/2015 2:15 PM  
**Deleted:** aggradation
- Kevin Schaefer 12/3/2015 2:16 PM  
**Deleted:** the frozen
- Kevin Schaefer 12/3/2015 2:16 PM  
**Comment [12]:** use consistent terms
- Kevin Schaefer 12/3/2015 2:16 PM  
**Deleted:** in it
- Kevin Schaefer 12/3/2015 2:16 PM  
**Deleted:** frozen
- Elchin Jafarov 12/19/2015 6:10 PM  
**Deleted:** The interactions between vegetat ... [11]
- Kevin Schaefer 12/3/2015 2:33 PM  
**Comment [13]:** I know what you were ... [13]
- Kevin Schaefer 12/3/2015 2:17 PM  
**Deleted:** This
- Elchin Jafarov 11/20/2015 11:14 AM  
**Formatted** ... [12]
- Kevin Schaefer 12/3/2015 2:17 PM  
**Deleted:** study emphasizes the importance ... [14]
- Elchin Jafarov 11/20/2015 11:14 AM  
**Formatted** ... [15]
- Elchin Jafarov 11/20/2015 11:14 AM  
**Formatted** ... [16]
- Elchin Jafarov 11/20/2015 11:14 AM  
**Formatted** ... [17]
- Elchin Jafarov 11/19/2015 5:29 PM  
**Moved up [2]:** Presence of the SOL impr ... [18]

717

718 **6. Acknowledgements**

719 This research was funded by NOAA grant NA09OAR4310063 and NASA grant NNX10AR63G.  
720 This work utilized the Janus supercomputer, which is supported by the National Science  
721 Foundation (award number CNS-0821794) and the University of Colorado Boulder. We thank  
722 K. Gregory at NSIDC for reviewing the manuscript. Software tools used in this study include  
723 m\_map MATLAB package and shadedErrorBar.m MATLAB script.

724

725 **7. References**

726 Ball, J. T.: An analysis of stomatal conductance, Ph.D. thesis, Stanford Univ., Stanford, Calif.,  
727 1988

728 Bonan, G. B.: A Land Surface Model (LSM Version 1.0) for ecological, hydrological, and  
729 atmospheric studies: Technical description and users guide, NCAR Tech. Note  
730 NCAR/TN-417+STR, Natl. Cent. for Atmos. Res., Boulder, Colo., 1996.

731 Brown, J., K. Hinkel and F. Nelson.: The 1 Circumpolar Active Layer Monitoring (CALM)  
732 program: Research designs and initial results. *Polar Geography*, 24,165-258,  
733 doi:10.1080/10889370009377698. 2000.

734 Brown, J., O. J. Ferrans Jr., J. A. Heginbottom, and E. S Melnikov, Eds.: Circum-Arctic Map of  
735 Permafrost and Ground-Ice Conditions. U.S. Geological Survey in Cooperation with the  
736 Circum-Pacific Council for Energy and Mineral Resources, Circum-Pacific Map Series  
737 CP-45, scale 1:10,000,000, 1 sheet, 1997

738 Brown, J., Hinkel, K.M.; Nelson, F.E.: The circumpolar active layer monitoring (CALM)  
739 program: Research designs and initial results. *Polar Geog.*, 24, 165–258, 2000.

740 Bonan, G. B.: A Land Surface Model (LSM Version 1.0) for ecological, hydrological, and  
741 atmospheric studies: technical description and users guide. NCAR Technical Note  
742 NCAR/TN-417+STR, Boulder, Colorado. 1996.

743 Burgess, M.M.; Smith, S.L.; Brown, J.; Romanovsky, V.; Hinkel, K. The Global Terrestrial  
744 Network for Permafrost (GTNet-P): Permafrost Monitoring Contributing to Global  
745 Climate Observations. Available online:  
746 [http://ftp2.cits.mcan.gc.ca/pub/geott/ess\\_pubs/211/211621/cr\\_2000\\_e14.pdf](http://ftp2.cits.mcan.gc.ca/pub/geott/ess_pubs/211/211621/cr_2000_e14.pdf).

747 Burke, EJ, IP Hartley, and CD Jones.: Uncertainties in the global temperature change caused by  
748 carbon release from permafrost thawing, *Cryosphere*, 6, 1063–1076, doi:10.5194/tc-6-  
749 1063-2012, 2012

750 Camill, P: Permafrost thaw accelerates in boreal peatlands during late-20th century climate  
751 warming *Clim. Change* 68 135–52. 2005

752 Callaghan, T.V., Johansson, M., Anisimov, O., Christiansen, H.H., Instanes, A., Romanovsky,  
753 V., and Smith, S.: Chapter 5: Changing permafrost and its impacts. In: *Snow, Water, Ice*  
754 *and Permafrost in the Arctic (SWIPA) 2011*. Arctic Monitoring and Assessment  
755 Programme (AMAP), Oslo, pp 62. 2011.

756 Chadburn, S., Burke, E., Essery, R., Boike, J., Langer, M., Heikenfeld, M., Cox, P., and  
757 Friedlingstein, P.: An improved representation of physical permafrost dynamics in the  
758 JULES land surface model, *Geosci. Model Dev. Discuss.*, 8, 715–759,  
759 doi:10.5194/gmdd-8-715-2015, 2015a.

760 Chadburn, S. E., Burke, E. J., Essery, R. L. H., Boike, J., Langer, M., Heikenfeld, M.,  
761 Cox, P. M., and Friedlingstein, P.: Impact of model developments on present and future  
762 simulations of permafrost in a global land-surface model, *The Cryosphere Discuss.*, 9,  
763 1965-2012, doi:10.5194/tcd-9-1965-2015, 2015b.

764 Collatz, G. J., J. T. Ball, C. Grivet, and J. A. Berry.: Physiological and environmental regulation  
765 of stomatal conductance, photosynthesis, and transpiration: A model that includes a  
766 laminar boundary layer, *Agric. For. Meteorol.*, 54, 107– 136, doi:10.1016/0168-  
767 1923(91)90002-8, 1991.

768 Collatz, G. J., M. Ribascarbo, and J. A. Berry.: Coupled photosynthesis-stomatal conductance  
769 model for leaves of C4 plants, *Aust. J. Plant Physiol.*, 19(5), 519–538, 1992.

770 Dutta, K., Schuur, E. A. G., Neff, J. C. and Zimov, S. A.: Potential carbon release from  
771 permafrost soils of Northeastern Siberia. *Global Change Biol.* 12, 2336–2351, 2006.

772 FAO, IIASA, ISRIC, ISS-CAS, and JRC: Harmonized World Soil Database (version 1.1) FAO,  
773 Rome, Italy and IIASA, Laxenburg, Austria, 2009.

774 Ekici, A., Chadburn, S., Chaudhary, N., Hajdu, L. H., Marmy, A., Peng, S., Boike, J., Burke, E.,  
775 Friend, A. D., Hauck, C., Krinner, G., Langer, M., Miller, P. A., and Beer, C.: Site-level  
776 model intercomparison of high latitude and high altitude soil thermal dynamics in tundra  
777 and barren landscapes, *The Cryosphere Discuss.*, 8, 4959-5013, doi:10.5194/tcd-8-4959-  
778 2014, 2014a.

779 Ekici, A., Beer, C., Hagemann, S., Boike, J., Langer, M., and Hauck, C.: Simulating high-  
780 latitude permafrost regions by the JSBACH terrestrial ecosystem model, *Geosci. Model  
781 Dev.*, 7, 631-647, doi:10.5194/gmd-7-631-2014, 2014b.

782 Farquhar, G. D., S. von Caemmerer, and J. A. Berry.: A biochemical model of photosynthetic  
783 CO<sub>2</sub> assimilation in leaves of C<sub>3</sub> species, *Planta*, 149, 78–90, doi:10.1007/BF00386231,  
784 1980.

785 Grøndahl L, Friberg T, Soegaard H.: Temperature and snow-melt controls on interannual  
786 variability in carbon exchange in the high Arctic. *Theor Appl Climatol* 88(1):111–125,  
787 2007.

788 Harden, J. W., Koven, C., Ping, C., Hugelius, G., McGuire D. A., Camill, P., Jorgenson, T.,  
789 Kuhry, P., Michaelson, G. J., O'Donnell, J.A., Schuur, E. A. G., Tarnocai C., Johnson,  
790 K., Grosse, G.: et al. (2012), Field information links permafrost carbon to physical  
791 vulnerabilities of thawing, *Geophys. Res. Lett.*, 39, L15704, doi:10.1029/2012GL051958.

792 Hugelius, G., Strauss, J., Zubrzycki, S., Harden, J. W., Schuur, E. A. G., Ping, C.-L.,  
793 Schirmer, L., Grosse, G., Michaelson, G. J., Koven, C. D., O'Donnell, J. A.,  
794 Elberling, B., Mishra, U., Camill, P., Yu, Z., Palmtag, J., and Kuhry, P.: Estimated stocks  
795 of circumpolar permafrost carbon with quantified uncertainty ranges and identified data  
796 gaps, *Biogeosciences*, 11, 6573–6593, doi:10.5194/bg-11-6573-2014, 2014.

797 Hugelius, G., Tarnocai, C., Broll, G., Canadell, J. G., Kuhry, P., and Swanson, D. K.: The  
798 Northern Circumpolar Soil Carbon Database: spatially distributed datasets of soil  
799 coverage and soil carbon storage in the northern permafrost regions, *Earth Syst. Sci.*  
800 *Data*, 5, 3–13, doi:10.5194/essd-5-3-2013, 2013.

801 Jafarov E E, Marchenko S S and Romanovsky V E.: Numerical modeling of permafrost  
802 dynamics in Alaska using a high spatial resolution dataset, *Cryosphere*, 6, 613–24, 2012.

803 Jafarov E.E., Nicolsky D.J., Romanovsky V.E., Walsh J.E., Panda S.K., Serreze M.C. 2014. The

804 effect of snow: How to better model ground surface temperatures. *Cold Regions Science*  
805 and *Technology*, Volume 102, Pages 63-77, ISSN 0165-232X, doi:  
806 10.1016/j.coldregions.2014.02.007.

807 Jafarov, E. E., Romanovsky V. E., Genet, H., McGuire A., D., Marchenko, S. S.: The effects of  
808 fire on the thermal stability of permafrost in lowland and upland black spruce forests of  
809 interior Alaska in a changing climate, *Environmental Research Letters*, 8, 035030, 2013.

810 Jackson, R. B., J. Canadell, J. R. Ehleringer, H. A. Mooney, O. E. Sala, and E. D. Schulze.: A  
811 global analysis of root distributions for terrestrial biomes, *Oecologia*, 108, 389–411,  
812 doi:10.1007/BF00333714, 1996.

813 Johnstone J F, Chapin F S III, Hollingsworth T N, Mack M C, Romanovsky V and Turetsky M.:  
814 Fire, climate change, and forest resilience in interior Alaska *Can. J. For. Res.*40 1302–12,  
815 2010.

816 Koven, C., P. Friedlingstein, P. Ciais, D. Khvorostyanov, G. Krinner, and C. Tarnocai.: On the  
817 formation of high-latitude soil carbon stocks: Effects of cryoturbation and insulation by  
818 organic matter in a land surface model, *Geophys. Res. Lett.*, 36, L21501,  
819 doi:10.1029/2009GL040150, 2009.

820 Koven, CD, B Ringeval, P Friedlingstein, P Ciais, P Cadule, D Khvorostyanov, G Krinner, and  
821 C Tarnocai.: Permafrost carbon-climate feedbacks accelerate global warming, *Proc. Natl.*  
822 *Acad. Sci. USA*, 108(36), 14769–14774, doi/10.1073/pnas.1103910108, 2011.

823 Koven, C.D., W.J. Riley, and A. Stern.: Analysis of permafrost thermal dynamics and response  
824 to climate change in the CMIP5 earth system models. *J. Climate*. 26:1877–1900.  
825 doi:10.1175/JCLI-D-12–00228.1, 2013.

826 Lawrence, D. M., and A. G. Slater.: Incorporating organic soil into a global climate model.  
827 *Climate Dynamics* 30(2-3): 145-160, doi:10.1007/s00382-007-0278-1, 2008.

828 MacDougall, AH, CA Avis and AJ Weaver.: Significant contribution to climate warming from  
829 the permafrost carbon feedback, *Nature Geosci.*, 5, 719-721, DOI: 10.1038/NGEO1573,  
830 2012.

831 Oberman, N.G.: Contemporary Permafrost Degradation of Northern European Russia. In:  
832 *Proceedings Ninth International Conference on Permafrost*. Vol. 2, 1305-1310 pp, 2008.

833 Oleson, K.W., Dai, Y., Bonan, G., Bosilovich, M., Dickinson, R., and coauthors.: Technical  
834 description of the Community Land Model (CLM). NCAR Tech. Note, TN-461+STR,  
835 174 pp, 2004.

836 Price, J. S., J. Cagampang, and E. Kellner.: Assessment of peat compressibility: is there an easy  
837 way? *Hydro. Processes*, 19, 3469–3475, 2005.

838 Sellers, PJ, DA Randall, GJ Collatz, JA Berry, CB Field, DA Dazlich, C Zhang, GD Collelo, L  
839 Bounoua.: A Revised Land Surface Parameterization of GCMs, Part I: Model  
840 Formulation, *J. Clim.*, 9(4), 676-705, 1996.

841 Schaefer, K., Collatz, G. J., Tans, P., Denning, A. S., Baker, I. and co-authors. : The combined  
842 Simple Biosphere/Carnegie-Ames-Stanford Approach (SiBCASA) Model. *J. Geophys.*  
843 *Res.*, 113, doi:10.1029/2007JG000603, 2008.

844 Schaefer, K. and Jafarov, E.: A parameterization of respiration in frozen soils based on substrate  
845 availability, *Biogeosciences Discuss.*, 12, 12027-12059, doi:10.5194/bgd-12-12027-2015,  
846 2015.

847 Schaefer, K., T. Zhang, L. Bruhwiler, and A. P. Barrett.: Amount and timing of permafrost

848 carbon release in response to climate warming, *Tellus Series B: Chemical and Physical*  
849 *Meteorology*, DOI: 10.1111/j.1600-0889.2011.00527.x, 2011.

850 Schaefer, K., Zhang, T., Slater, A. G., Lu, L., Etringer, A. and Baker, I.: Improving simulated  
851 soil temperatures and soil freeze/thaw at high-latitude regions in the Simple  
852 Biosphere/Carnegie-Ames-Stanford Approach model. *J. Geophys. Res.*, 114,  
853 doi:10.1029/2008JF001125, 2009.

854 Schaefer, K, H Lantuit, VE Romanovsky, EAG Schuur, and R Witt .: The impact of the  
855 permafrost carbon feedback on global climate, *Env. Res. Lett.*, 9, 085003 (9pp)  
856 doi:10.1088/1748-9326/9/8/085003, 2014.

857 Shiklomanov, N.I.; Streletskiy, D.A.; Nelson, F.E.; Hollister, R.D.; Romanovsky, V.E.; Tweedie,  
858 C.E.; Bockheim, J.G.; Brown, J. Decadal variations of active-layer thickness in moisture-  
859 controlled landscapes, Barrow, Alaska. *J. Geophys. Res.* 115, G00I04, 2010.

860 E. A. G. Schuur, A. D. McGuire, C. Schädel, G. Grosse, J. W. Harden, D. J. Hayes, G. Hugelius,  
861 C. D. Koven, P. Kuhry, D. M. Lawrence, S. M. Natali, D. Olefeldt, V. E. Romanovsky,  
862 K. Schaefer, M. R. Turetsky, C. C. Treat and J. E. Vonk.: Climate change and the  
863 permafrost carbon feedback. *Nature* 520, 171–179. doi:10.1038/nature14338, 2015.

864 Smith, S., and M.M. Burgess.: Ground Temperature Database for Northern Canada. Geological  
865 Survey of Canada Open File Report No. 3954. 28 pages, 2000.

866 Tarnocai, C., Canadell, J. G., Schuur, E. A. G., Kuhry, P., Mazhitova, G. and Zimov, S.: Soil  
867 organic carbon pools in the northern circumpolar permafrost region. *Global Biogeochem.*  
868 *Cycles*, 23, doi:10.1029/2008GB003327, 2009.

869 Tryon, P., Chapin, F. III.: Tem- perature controls over root growth and root biomass in taiga



870 forest trees. *Can. J. For. Res.* 13:827-33, 1983.

871 Van Cleve, K.L., Oliver, L., Schlentner, R., Viereck, L. and Dyrness, C.T.: Productivity and  
872 nutrient cycling in taiga forest ecosystems. *Can. J. For. Res.*, 13: 747-766, 1983.

873 Vidale, P.L., R Stockli.: Prognostic canopy air space solutions for land surface exchanges, *Theor.*  
874 *Appl. Climatol.*, 80, 245-257, 2005.

875 Yi S, Manies K, Harden J and McGuire A D.: Characteristics of organic soil in black spruce  
876 forests: implications for the application of land surface and ecosystem models in cold  
877 regions *Geophys. Res. Lett.* 36 L05501, 2009.

878 Yi, S., A. D. McGuire, E. Kasischke, J. Harden, K. L. Manies, M. Mack, and M. R. Turetsky  
879 (2010), A Dynamic organic soil biogeochemical model for simulating the effects of  
880 wildfire on soil environmental conditions and carbon dynamics of black spruce forests, *J.*  
881 *Geophys. Res.*, 115, G04015, doi:10.1029/2010JG001302.

882 Yuan, F., S. Yi, A. D. McGuire, K. H. Johnsen, J. Liang, J. Harden, E. Kasischke, and W. Kurz  
883 (2012), Assessment of historical boreal forest C dynamics in Yukon River Basin:  
884 Relative roles of warming and fire regime change, *Ecol. Appl.*, 22, 2091-2109.

885

886 Wei, Y., Liu, S., Huntzinger, D. N., Michalak, A. M., Viovy, N., Post, W. M., Schwalm, C. R.,  
887 Schaefer, K., Jacobson, A. R., Lu, C., Tian, H., Ricciuto, D. M., Cook, R. B., Mao, J., and  
888 Shi, X.: The North American Carbon Program Multi-scale Synthesis and Terrestrial  
889 Model Intercomparison Project: Part 2 - Environmental Driver Data. *Geoscientific Model*  
890 *Development*, 7, 2875-2893, doi:10.5194/gmd-7-2875-2014, 2014.

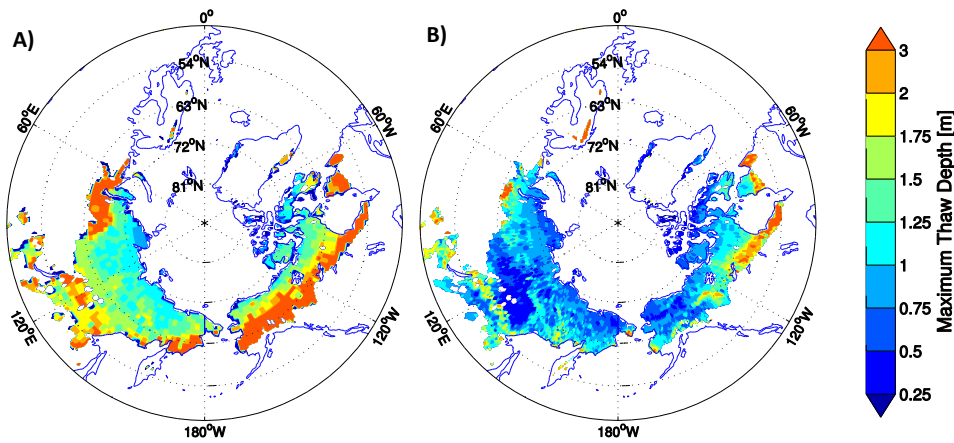
891 Wipf, S., and Rixen, C.: A review of snow manipulation experiments in Arctic and alpine tundra

892 ecosystems. *Polar Res* 29(1):95–109. doi:10.1111/j.1751-8369.2010.00153.x, 2010.

893 Zhang, T.: Influence of the seasonal snow cover on the ground thermal regime: An overview,

894 *Rev. Geophys.*, 43, RG4002, doi:10.1029/2004RG000157, 2005.

895



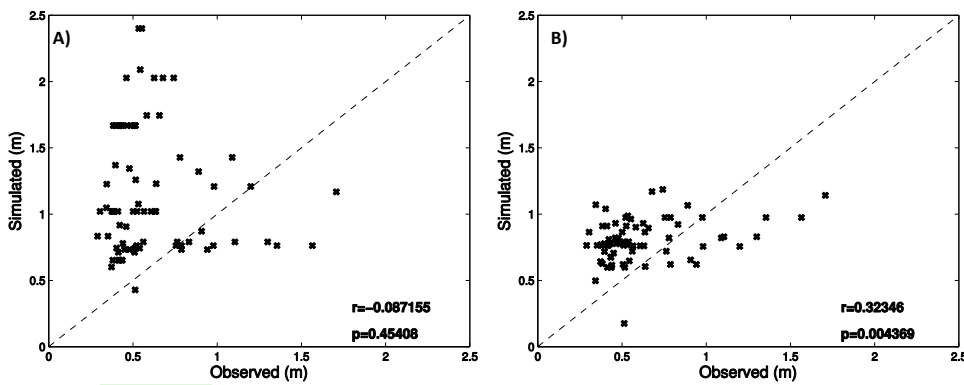
896

897 **Figure 1.** Maximum thaw depth averaged over last five years after spinup from A) Schaefer et al., (2011)  
 898 and B) this study, in meters.

899

Kevin Schaefer 12/3/2015 1:51 PM

Comment [14]: Add titles to panels a and b



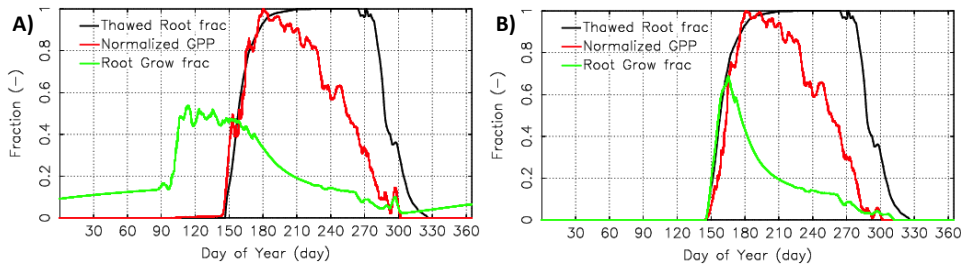
900

901 **Figure 2.** Comparison of the mean active layer thickness (ALT) from 76 Circumpolar Active Layer  
 902 Monitoring stations with the averaged ALT from last five years after spinup with A) Schaefer et al., (2011)  
 903 and B) this study.  $r$  is a Pearson's correlation coefficient and  $p$  is a significance value,  $p < 0.05$  stands for  
 904 the 95% of confidence.

905

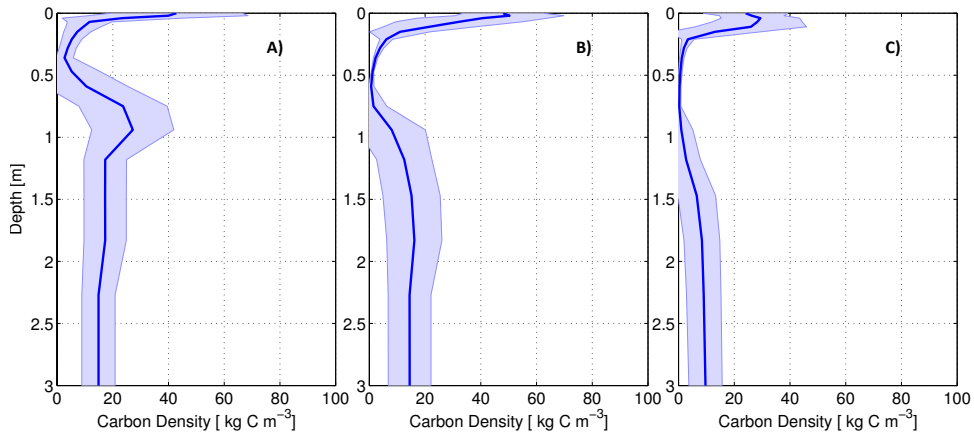
Kevin Schaefer 12/3/2015 1:51 PM

Comment [15]: Add titles to panels a and b



906

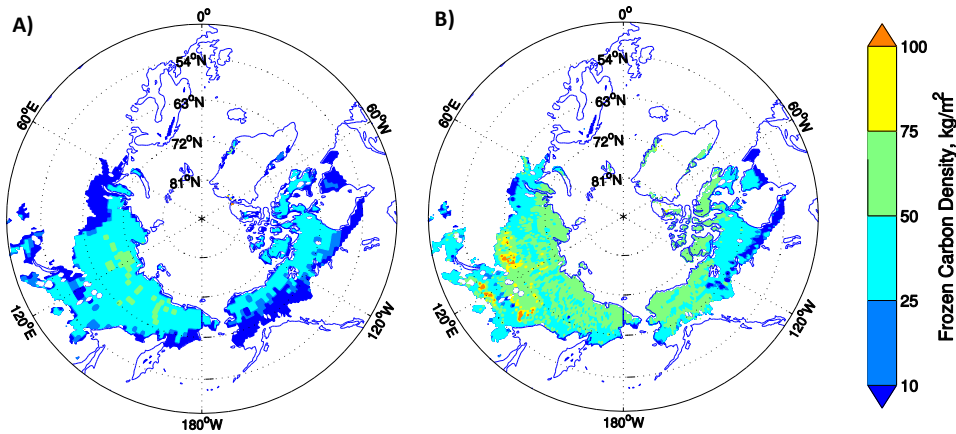
907 **Figure 3:** A) and B) root growth without and with the frozen soil constraint on growth.



908

909 **Figure 4.** An averaged soil carbon distribution from 200 grid cells A) for the tundra region in continuous  
 910 permafrost zone, B) for the boreal forest on the boundary between continuous and discontinuous zones,  
 911 and C) for the low carbon soil at the south border of the discontinuous permafrost zone. The solid blue  
 912 curve indicates the mean the white blue shading indicate the spread in the soil carbon density.  
 913

Elchin Jafarov 11/19/2015 6:10 PM  
 Deleted: 5

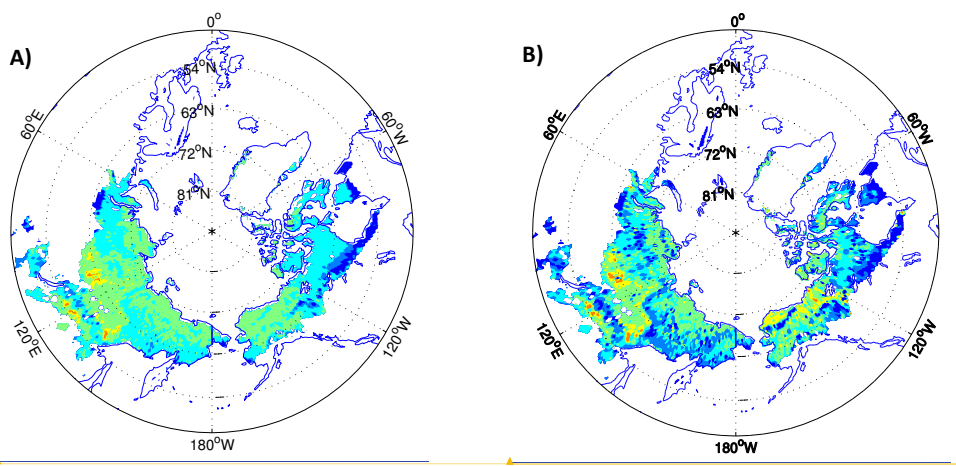


915

916 | **Figure 5.** The frozen carbon maps obtained assuming uniform frozen carbon distribution at the initial time  
 917 step, and averaged over five years at the end of the steady state run: A) from Schaefer et al., (2011), and  
 918 B) from the current run, correspondingly.

919

Elchin Jafarov 11/19/2015 6:11 PM  
 Deleted: 6



Unknown  
 Formatted: Font:(Default) Times New  
 Unknown  
 Formatted: Font:(Default) Times New  
 Elchin Jafarov 11/20/2015 9:25 AM  
 Formatted Table

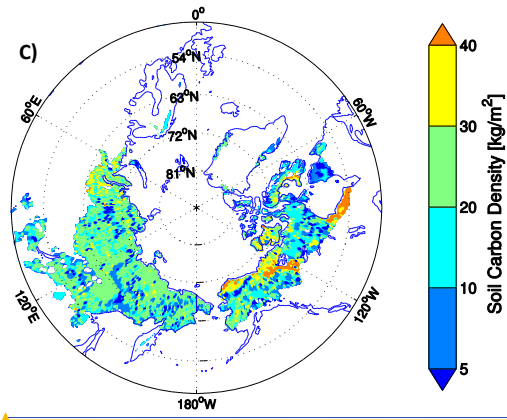


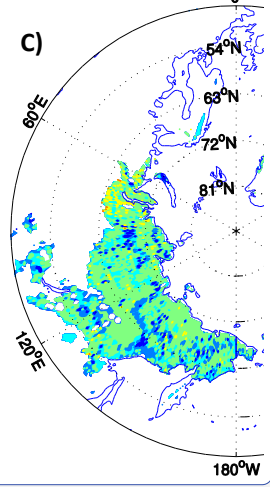
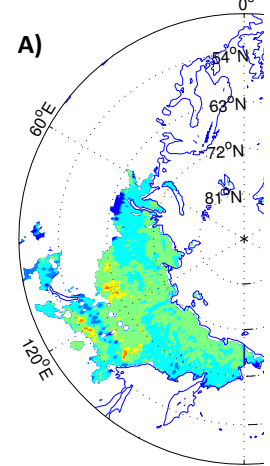
**Figure 6.** The soil carbon maps averaged over top 3 meters: A) from SiBCASA at the end of the steady state run, with constant permafrost density, B) from SiBCASA at the end of the steady state run, with non-constant permafrost density, and C) from the NCSCDv2, correspondingly.

921

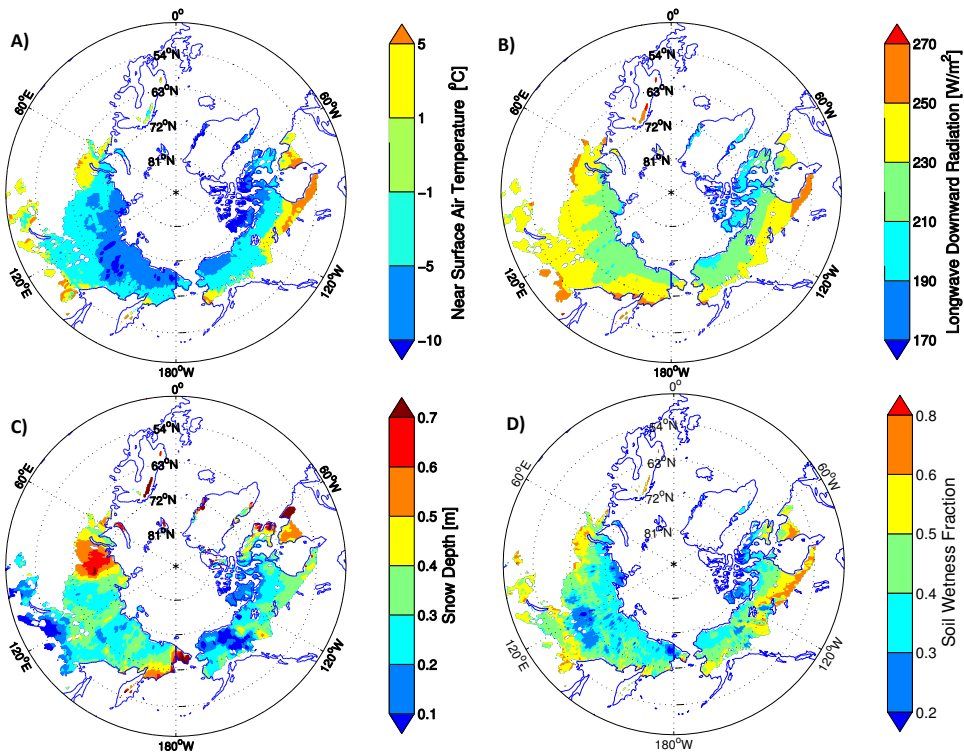
922

Unknown  
 Formatted: Font:(Default) Times New  
 Elchin Jafarov 11/19/2015 7:52 PM  
 Formatted: Space Before: 0 pt, After: 0 pt, Line spacing: single  
 Elchin Jafarov 11/19/2015 7:53 PM  
 Formatted: Font:(Default) Arial, 10 pt  
 Elchin Jafarov 11/19/2015 7:53 PM  
 Formatted: Font:(Default) Arial, 10 pt  
 Elchin Jafarov 11/19/2015 6:12 PM  
 Comment [16]: Need to change the number

Elchin Jafarov 11/19/2015 7:49 PM



Deleted:  
 Unknown  
 Formatted: Font:(Default) Times New Roman



924

925 | **Figure 7.** A) The near air temperature for averaged over first two month of the fall season. B) The  
 926 | downwelling long-wave radiation, averaged yearly over 10 years. C) The maximum snow depth obtained over  
 927 | 10 years for the steady state run, and D) the soil wetness fraction (dimensionless fraction of 1),  
 928 | representing overall near-surface soil wetness, averaged yearly over 10 years.

929 |

930

Elchin Jafarov 11/19/2015 6:11 PM  
 Deleted: 8  
 Elchin Jafarov 11/19/2015 6:11 PM

**Plot A:** Thaw Depth [m] vs. Near Surface Air Temperature [°C].  
 Equation:  $y = 0.06x + 1.24$   
 Correlation:  $R = 0.62$

**Plot C:** Thaw Depth [m] vs. Soil Wetness Fraction.  
 Equation:  $y = 0.43x + 0.93$   
 Correlation:  $R = 0.11$

Deleted:  
 Unknown  
 Formatted: Font:(Default) Times New Roman